Operation of Grid-Connected DFIG Under Unbalanced Grid Voltage Condition

Yi Zhou, *Student Member, IEEE*, Paul Bauer, *Senior Member, IEEE*, Jan A. Ferreira, *Fellow, IEEE*, and Jan Pierik

***Abstract*—Doubly fed induction generator (DFIG) still shares a large part in today's wind power market. It provides the benefits of variable speed operation cost-effectively, and can control its active and reactive power independently. Crowbar protection is often adopted to protect the rotor-side voltage source converter (VSC) from transient overcurrent during grid voltage dip. But under unbalanced grid voltage condition, the severe problems are not the transient overcurrent, but the electric torque pulsation and dc voltage ripple in the back-to-back VSCs. This paper develops dynamic models in MATLAB/Simulink, validates it through experiments, investigates the behavior of DFIG during unbalanced grid voltage condition, and proposes new controllers in separated positive and negative sequence. Methods to separate positive and negative sequence components in real time are also developed, and their responses to unsymmetrical voltage dip are compared. Simulation results prove that the separated positive and negative sequence controllers limit the torque pulsation and dc voltage ripple effectively.**

***Index Terms*—Control, doubly fed induction generator (DFIG), operation, unbalanced.**

I. Introduction

THE installed capacity of wind power in Europe reached approximately 33,600 MW until the end of 2004. The demand for connecting large-scale wind parks to the power grid is still on the rise. The increasing size of wind turbine and wind park resulted in new interconnection rules or grid codes. Today, there is a need to control wind power, both in active and reactive power, and to be able to stay connected with the grid when grid faults happen. The doubly fed induction generator (DFIG) has the largest world market share of wind turbine concepts since the year 2002 [1], because of its ability to provide variable speed operation and independent active and reactive power control in a cost-effective way. As DFIG's stator is directly connected with ac grid, it has poor low-voltage ride through (LVRT) capability due to the poorly damped flux oscillations during grid voltage dip. Many studies have been conducted on the LVRT capability of DFIG [3]–[6], [9], with most of them focused on the behavior and protection of DFIG under symmetrical fault. During the symmetrical fault, transient overcurrent in the rotor is identified as the most severe LVRT problem of the DFIG, because the rotor-side voltage source converter (VSC) is very sensitive to thermal overload. Thus, the active crowbar protection is designed to short-circuit the rotor under symmetrical grid voltage dip, both to protect the rotor-side VSC and to damp out the oscillations faster. In reality, however, unsymmetrical fault happens much more frequently than symmetrical fault. Furthermore, it is identified that the unbalanced voltages can occur in a weak power grid even during normal operation [7], [8], [16], [17]. Under the unbalanced grid voltage, the most severe operation problem of DFIG may not be the transient overcurrent, but the large electric torque pulsation that causes wear and tear of the gearbox, and large voltage ripple in the dc link of back-to-back VSC that may decrease the lifetime of the dc capacitance. Literatures [10], [11] define the instantaneous active and reactive power that can be used to design and operate the grid-connected VSC under unbalanced grid situations [12]–[15]. Literatures [16], [17], [19] on the control system of DFIG under unbalanced grid voltage condition [16] used a feedforward loop on the classical-field-oriented current (FOC) controller to limit torque ripple, which was simple and robust. But its performance depended on the filter. In [17], the grid VSC was controlled as a STATCOM and supplied reactive power to compensate the unbalanced grid voltage. Its performance depended on the current ratings of grid VSC and impedance between generator terminal and fault location. However, a theoretical analysis of DFIG under unsymmetrical fault is still missing, and a systematic approach to limit both torque pulsation and dc voltage ripple is required. In this paper, the behavior of DFIG under unbalanced grid voltage is thoroughly analyzed, and a dual-sequence FOC controller is proposed. The rotor VSC is controlled to limit the torque pulsation, and the grid VSC is controlled to limit the dc voltage ripple. A dynamic model of DFIG is made in MATLAB/Simulink. Simulation results prove the effectiveness of the proposed control system.

II. DFIG System Description, Modeling, and Verification

A. System Description

Fig. 1 describes the DFIG system and the proposed controllers. Rotor VSC and grid VSC are both controlled in positive and negative sequences. According to symmetrical components theory [2], during unbalanced voltage dip, the system can be decoupled into positive, negative, and zero sequence. The positive and negative sequences are balanced three-phase systems, which can be transferred to positive dq and negative dq system. Their voltages and currents are dc values at steady state, thus a simple PI controller can be used.

Manuscript received November 12, 2007; revised April 15, 2008. First published February 2, 2009; current version published February 19, 2009. This work was supported in part by the Project PhD@Sea, which was substantially funded under the BSIK Program of the Dutch Government, and by the consortium WE@Sea. Paper no. TEC-00424-2007.

Y. Zhou, P. Bauer, and J. A. Ferreira are with the Electrical Power Processing Group, Delft University of Technology, Delft 2628CD, The Netherlands (e-mail: yi.zhou@tudelft.nl).

J. Pierik is with the Energy Research Center of Netherlands, Petten 1755ZG, The Netherlands (e-mail: pierik@ecn.nl).

Digital Object Identifier 10.1109/TEC.2008.2011833

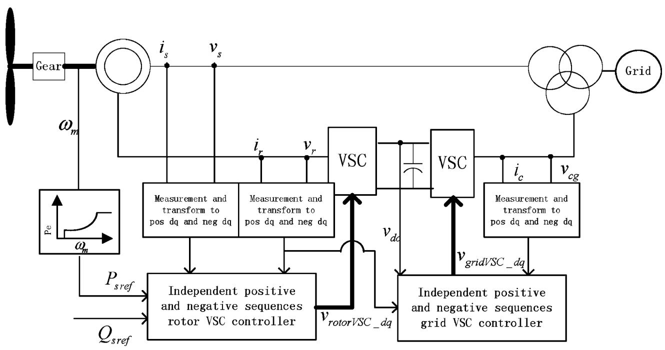

Fig. 1. Simplified diagram of DFIG system with proposed controllers.

Following assumptions are required to fully decouple positive and negative sequences.

1) DFIG's stator and rotor windings are assumed to be symmetrical.
2) Grid VSC's three-phase ac inductances and resistances are symmetrical.

The reference stator currents and grid converter currents are calculated according to instantaneous reactive power theory [10], [11]. Here, only a three-phase three-wire system is studied, where zero sequence is omitted. The choice is justified by the following reasons.

1) The transformer is often Y/Δ connected.
2) The neutral point of stator winding of DFIG is not grounded.

In the following sections, the simulation results of DFIG under symmetrical and unsymmetrical voltage dips will be presented first, and then instantaneous reactive power theory will be used to analyze the behavior of DFIG.

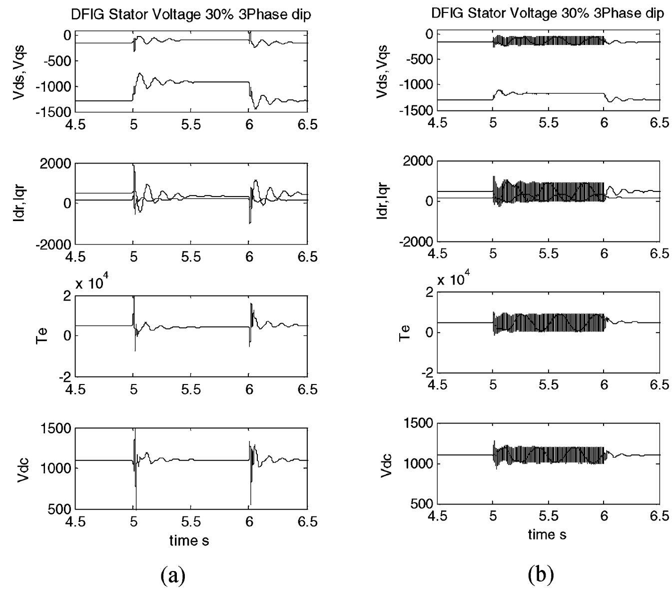

Fig. 2. Simulation results of DFIG under (a) symmetrical and (b) unsymmetrical voltage dips. Graphs from top to bottom are stator voltages, rotor currents, electric torques, and dc voltages, respectively.

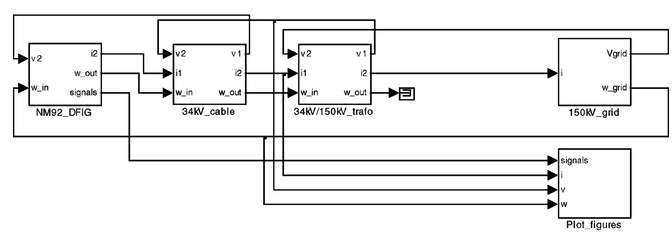

Fig. 3. Simulink model of DFIG system.

B. Symmetrical and Unsymmetrical Voltage Dip

Simulation results of DFIG under symmetrical and unsymmetrical voltage dips are shown in Fig. 2.

Fig. 2(a) shows that under symmetrical voltage dip, the most severe problem is the transient overcurrent in the rotor. This overcurrent problem is generally protected by the so-called "active crowbar protection," which uses thyristor-controlled resistor bank to short-circuit the rotor windings.

Fig. 2(b) shows that under unsymmetrical voltage dip, the maximum rotor currents can be smaller, but have 100 Hz oscillations, and cause large torque ripple and dc voltage ripple. It is worth noting that the magnitude of rotor current oscillation depends on the moment of voltage dip. The starting moment of the voltage dip determines the initial conditions of the stator currents, and thus determines the natural response of the stator currents. The natural response of stator currents has a large influence on the transient rotor currents.

C. Modeling and Validation

The complete DFIG system is modeled in MATLAB/Simulink. These models are developed in the synchronous rotating *dq* reference frame in order to improve the simulation speed, because the balanced three-phase voltage and current in the synchronous rotating *dq* reference frame are dc values at steady state. The Simulink model of DFIG system is shown in Fig. 3.

Experimental data to verify the DFIG Simulink model was provided by Chalmers University [18], and the Simulink model will be used to prove the effect of the proposed new controller. Both symmetrical and unsymmetrical voltage dips were applied on the terminal of a 850 kW DFIG, as shown in Fig. 4. The parameters of the DFIG are listed in Table I.

In Figs. 4 and 5, before 2.0 s, the DFIG was under normal operation. Then, between 2.0 and 2.1 s, unsymmetrical voltage dip was applied, which lasts about 0.1 s. Thereafter, symmetrical voltage dip was applied between 2.1 and 2.2 s, which lasts about 0.1 s. Finally, after 2.2 s, DFIG's terminal voltage was recovered to normal value. The measured stator voltage dips were applied on the terminal of DFIG in the simulink model. Simulation result were compared with measurement in Fig. 5, which shows good agreement between simulated and measured active power of DFIG during both unsymmetrical and symmetrical voltage dips.

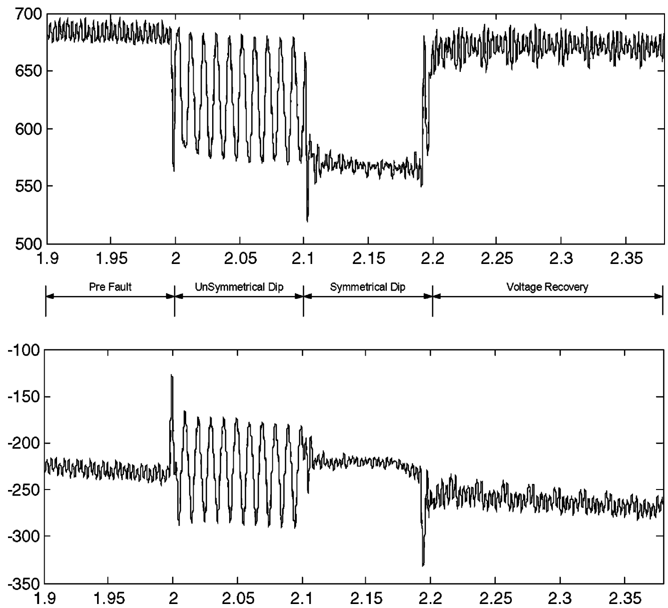

Fig. 4. Stator voltage dips of DFIG.

TABLE I
PARAMETERS OF THE 850-KW DFIG

Rs	Lls	Rr	Llr	Lms	Lmr
1.2e-3	1.18e-4	5.2e-3	3.08e-4	4.6e-3	1.82e-2

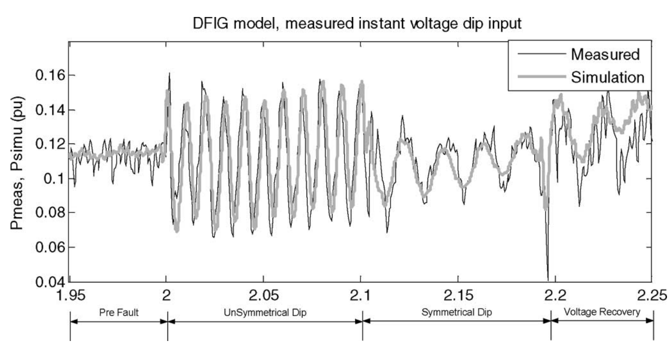

Fig. 5. Compare measured and simulated active power of DFIG under unsymmetrical and symmetrical voltage dip; solid green line—measurement and dotted blue line—simulation.

III. REACTIVE POWER THEORY AND SIGNAL EXTRACTION

A. Instantaneous Reactive Power Theory

According to instantaneous reactive power theory [10], the instantaneous power p and q in stationary $\alpha\beta$ reference frame are

$$\begin{bmatrix} p \\ q \end{bmatrix} = \begin{bmatrix} v_\alpha i_\alpha + v_\beta i_\beta \\ v_\beta i_\alpha - v_\alpha i_\beta \end{bmatrix}. \tag{1}$$

Equation (1) is true for both balanced and unbalanced three-phase three-line system. The stationary $\alpha\beta$ reference frame can be decoupled into positive and negative sequences as

$$\begin{bmatrix} v_\alpha(t) \\ v_\beta(t) \end{bmatrix} = \begin{bmatrix} v_\alpha^+(t) + v_\alpha^-(t) \\ v_\beta^+(t) + v_\beta^-(t) \end{bmatrix}. \tag{2}$$

Using Equations (1) and (2) and Park's transformation, the instantaneous active and reactive power of positive and negative dq sequences can be derived as

$$\begin{aligned} \begin{bmatrix} p \\ q \end{bmatrix} = \begin{bmatrix} \bar{p} + \tilde{p} \\ \bar{q} + \tilde{q} \end{bmatrix} &= \begin{bmatrix} (v_d^+ i_d^+ + v_q^+ i_q^+ + v_d^- i_d^- + v_q^- i_q^-) \\ (v_q^+ i_d^+ - v_d^+ i_q^+ + v_q^- i_d^- - v_d^- i_q^-) \end{bmatrix} \\ &+ \sin(2\theta) \begin{bmatrix} (v_d^+ i_q^- - v_q^+ i_d^- + v_q^- i_d^+ - v_d^- i_q^+) \\ (v_d^+ i_d^- + v_q^+ i_q^- + v_d^- i_d^+ + v_q^- i_q^+) \end{bmatrix} \\ &+ \cos(2\theta) \begin{bmatrix} v_d^+ i_d^- + v_q^+ i_q^- + v_d^- i_d^+ + v_q^- i_q^+ \\ v_d^+ i_q^- - v_q^+ i_d^- + v_q^- i_d^+ - v_d^- i_q^+ \end{bmatrix}. \end{aligned} \tag{3}$$

The terms of $\sin(2\theta)$ and $\cos(2\theta)$ in (3) are the oscillation parts of instantaneous power p and q. The oscillation parts of instantaneous active power p will cause dc voltage ripple and electric torque pulsation, such as shown in simulation results of DFIG in Fig. 2.

In order to limit the dc voltage ripple or torque pulsation under unsymmetrical voltage dip, the terms of $\sin(2\theta)$ and $\cos(2\theta)$ of instantaneous active power p in (3) have to be controlled to zero. Rearranging (3), four independent equations can be used to determine the four reference currents $i_d^+, i_q^+, i_d^-, i_q^-$, and the currents can be controlled by voltages of VSC $v_d^+, v_q^+, v_d^-, v_q^-$ with simple PI controllers

$$\begin{bmatrix} \bar{p} \\ \bar{q} \\ \tilde{p}_{\sin 2\theta} \\ \tilde{p}_{\cos 2\theta} \end{bmatrix} = \begin{bmatrix} P_{\mathrm{ref}} \\ Q_{\mathrm{ref}} \\ 0 \\ 0 \end{bmatrix} = \begin{bmatrix} v_d^+ i_d^+ + v_q^+ i_q^+ + v_d^- i_d^- + v_q^- i_q^- \\ v_q^+ i_d^+ - v_d^+ i_q^+ + v_q^- i_d^- - v_d^- i_q^- \\ v_d^+ i_q^- - v_q^+ i_d^- + v_q^- i_d^+ - v_d^- i_q^+ \\ v_d^+ i_d^- + v_q^+ i_q^- + v_d^- i_d^+ + v_q^- i_q^+ \end{bmatrix}. \tag{4}$$

$\tilde{p}_{\sin 2\theta}$ and $\tilde{p}_{\cos 2\theta}$ are the two oscillating terms of instantaneous active power p. In order to control them to zero, instantaneous voltage and current have to be separated to positive and negative sequences in real time.

B. Real-Time Signal Processing

The proposed control method requires fast and accurate separation of positive and negative sequences. Two methods are often used [12].

The first method is based on the fact that the negative sequence component appears as a second-order harmonic in the synchronous rotating frame—positive *dq*, and the positive sequence component appears as a second-order harmonic in the negative synchronous rotating frame—negative *dq*. The low-pass filter can be used to bypass the dc values and suppress the high-frequency oscillations. Thus, the positive and negative sequences are separated in real time. The description of this method is shown in Fig. 6.

The second method is the so-called "signal delay cancellation" method (see Fig. 7). The abc system is first transformed into stationary $\alpha\beta$ reference frame using Clark's transformation, then it is delayed for $T/4$. The positive and negative sequences can be calculated by adding or subtracting the present real-time signal with the delayed signal. It is explained mathematically in the following way.

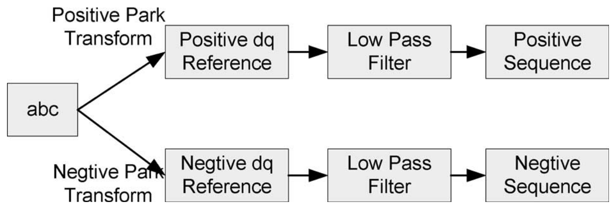

Fig. 6. Separate positive and negative sequences by low-pass filters.

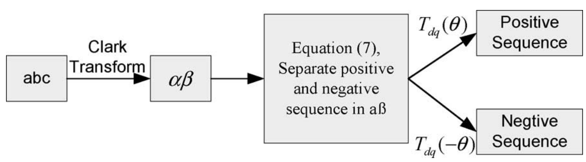

Fig. 7. Separate positive and negative sequences by "signal delay cancellation" method.

The abc system can be transformed into stationary $\alpha\beta$ reference frame using Clark's transformation, and can be expressed in positive and negative sequences as

$$\begin{bmatrix} v_\alpha(t) \\ v_\beta(t) \end{bmatrix} = \begin{bmatrix} v_\alpha^+(t) + v_\alpha^-(t) \\ v_\beta^+(t) + v_\beta^-(t) \end{bmatrix} = \begin{bmatrix} v^+\cos(\omega t + \phi^+) + v^-\cos(-\omega t + \phi^-) \\ v^+\sin(\omega t + \phi^+) + v^-\sin(-\omega t + \phi^-) \end{bmatrix}. \tag{5}$$

Delaying this signal for T/4

$$\begin{bmatrix} v_\alpha\left(t - \frac{T}{4}\right) \\ v_\beta\left(t - \frac{T}{4}\right) \end{bmatrix} = \begin{bmatrix} v^+\sin(\omega t + \phi^+) - v^-\sin(\omega t + \phi^-) \\ -v^+\cos(\omega t + \phi^+) + v^-\cos(-\omega t + \phi^-) \end{bmatrix}. \tag{6}$$

From equations of $\alpha\beta(t)$ (5) and $\alpha\beta(t - T/4)$ (6), the positive and negative sequences can be calculated

$$\begin{bmatrix} v_\alpha^+(t) \\ v_\beta^+(t) \\ v_\alpha^-(t) \\ v_\beta^-(t) \end{bmatrix} = \frac{1}{2} \begin{bmatrix} 1 & 0 & 0 & -1 \\ 0 & 1 & 1 & 0 \\ 1 & 0 & 0 & 1 \\ 0 & 1 & -1 & 0 \end{bmatrix} \cdot \begin{bmatrix} v_\alpha(t) \\ v_\beta(t) \\ v_\alpha(t - T/4) \\ v_\beta(t - T/4) \end{bmatrix}. \tag{7}$$

The positive and negative sequences in stationary $\alpha\beta$ reference frame can be further transformed into positive *dq* and negative *dq* sequences using

$$\begin{bmatrix} v_d^+(t) \\ v_q^+(t) \end{bmatrix} = \begin{bmatrix} \cos\theta & \sin\theta \\ -\sin\theta & \cos\theta \end{bmatrix} \cdot \begin{bmatrix} v_\alpha^+(t) \\ v_\beta^+(t) \end{bmatrix}$$
$$\begin{bmatrix} v_d^-(t) \\ v_q^-(t) \end{bmatrix} = \begin{bmatrix} \cos(-\theta) & \sin(-\theta) \\ -\sin(-\theta) & \cos(-\theta) \end{bmatrix} \cdot \begin{bmatrix} v_\alpha^-(t) \\ v_\beta^-(t) \end{bmatrix}. \tag{8}$$

At the moment of voltage dip and/or recovering, the "signal delay cancellation" method will have large transients and also a time delay of $T/4$. This method is summarized in Fig. 7.

The unbalanced voltages in the positive synchronous rotating *dq* reference frame, with and without applying those two separation methods, are shown in Fig. 8.

Without the two separation methods, the unbalanced three-phase voltage or current has second-order harmonics in the positive synchronous rotating *dq* reference frame. Both separation methods have time delays before their outputs can reach steady states. The "signal delay cancellation" is much faster than the "low-pass filter" method, but it has larger oscillation magnitudes at the start and end period of voltage dip.

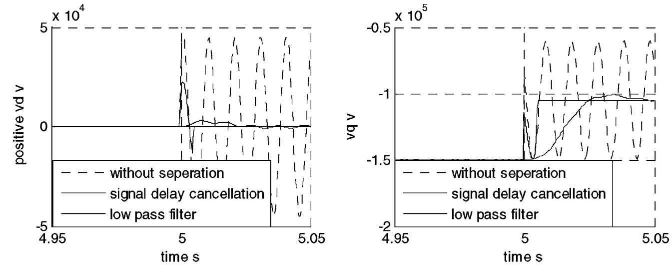

(a) (b)

Fig. 8. Unbalanced voltages in positive *dq* reference frame with and without using the two separation methods (a) vd and (b) vq.

IV. Dual Sequences—Positive and Negative Sequences Field-Oriented Current Controller

A. Control of Rotor VSC

Assuming the DFIG itself is symmetric, the voltage equations of positive and negative *dq* sequences in generator convention are listed as in (9).

In (9), ω_s is the stator electrical angular velocity, and ω_r is the rotational speed of rotor times the number of pole pairs $\omega_m \cdot$p

$$\begin{bmatrix} v_{ds}^\pm \\ v_{qs}^\pm \\ v_{dr}^\pm \\ v_{qr}^\pm \end{bmatrix} = \begin{bmatrix} -R_s i_{ds}^\pm - (\pm\omega_s \Psi_{qs}^\pm) + \frac{d\Psi_{ds}^\pm}{dt} \\ -R_s i_{qs}^\pm + (\pm\omega_s \Psi_{ds}^\pm) + \frac{d\Psi_{qs}^\pm}{dt} \\ -R_r i_{dr}^\pm - (\pm\omega_s - \omega_r)\Psi_{qr}^\pm + \frac{d\Psi_{dr}^\pm}{dt} \\ -R_r i_{dr}^\pm + (\pm\omega_s - \omega_r)\Psi_{dr}^\pm + \frac{d\Psi_{qr}^\pm}{dt} \end{bmatrix}. \tag{9}$$

The positive and negative sequences are completely decoupled as shown in (9), thus the DFIG can be controlled in positive and negative *dq* sequences independently.

The controller of rotor VSC is designed from (9), which uses rotor voltages to control stator currents, and uses stator currents to control active and reactive power as shown in Fig. 9.

In rotor VSC controller, the cross-coupling terms between d and q are $(\pm\omega_s - \omega_r)\Psi_{qr}^\pm$ and $(\pm\omega_s - \omega_r)\Psi_{dr}^\pm$. They are different in positive and negative sequences. In order to completely decouple d- and q-axes, these cross-coupling terms are feedforwarded and added with the outputs of PI controllers.

B. Control of Grid VSC

Assuming the smoothing ac inductance and resistance of grid VSC is balanced, the voltage equations of positive and negative *dq* sequences are

$$\begin{bmatrix} v_{dc}^\pm \\ v_{qc}^\pm \end{bmatrix} = \begin{bmatrix} v_{dg}^\pm + R_c i_{dc}^\pm + (\pm\omega_s L_c i_{qc}^\pm) + L_c \frac{di_{dc}^\pm}{dt} \\ v_{qg}^\pm + R_c i_{qc}^\pm - (\pm\omega_s L_c i_{dc}^\pm) + L_c \frac{di_{qc}^\pm}{dt} \end{bmatrix}. \tag{10}$$

Unlike the normal VSC under unbalanced voltage dip [12], [13], the dc voltage ripple of DFIG is caused by both the rotor VSC and grid VSC. Thus, the instantaneous active power of grid VSC has to be controlled in coordination with the rotor VSC, in

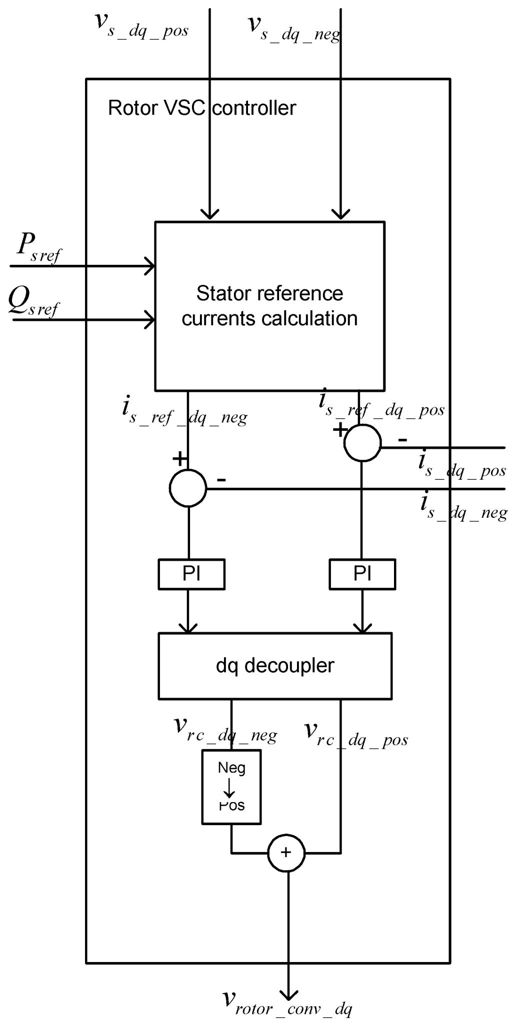

Fig. 9. Dual sequence current controller of rotor VSC.

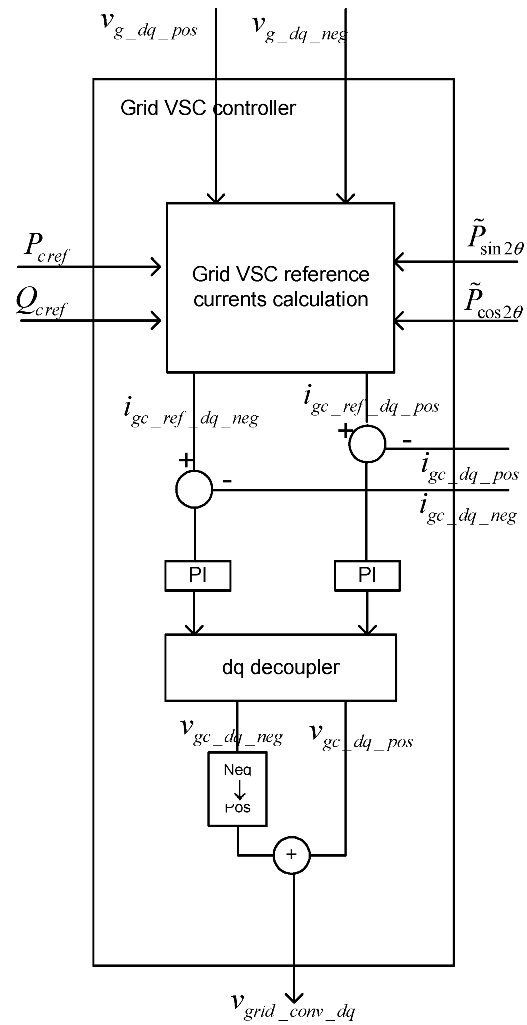

Fig. 10. Dual sequence current controller of grid VSC.

order to eliminate the dc voltage ripple. A feedforward loop is used to compensate rotor oscillation power $\tilde{p}_{\sin 2\theta}$ and $\tilde{p}_{\cos 2\theta}$.

The reference currents of grid VSC are calculated from dc link voltage, grid ac voltage, rotor oscillation power, and reference reactive power Q_{ref}. The details of this controller can be seen in Fig. 10.

In grid VSC controller, the cross-coupling terms between d and q are $(\pm\omega_s L_c i_{qc}^{\pm})$ and $(\pm\omega_s L_c i_{dc}^{\pm})$. Similar to that in the rotor VSC controller, they are feedforwarded and added with outputs of PI controllers.

C. Simulation Results of Dual Sequences Controller

The effects of the proposed dual sequence FOC controllers can be seen in Fig. 11.

The new controller of rotor VSC limits the torque pulsation to less than 20% of the original value, and the grid VSC limits the dc voltage ripple.

Effects of classical FOC and dual sequence FOC can be seen clearly in Fig. 12.

When the dual sequence FOC is applied on the rotor VSC, the stator power oscillation is limited, but the rotor power

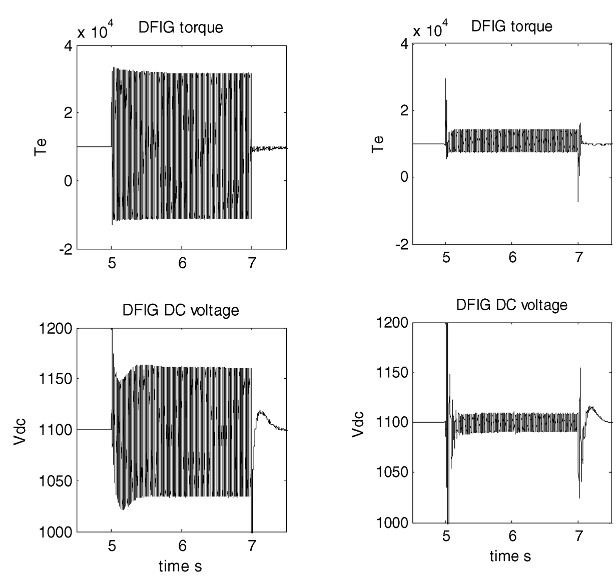

(a) (b)

Fig. 11. Compare the responses of DFIG under unsymmetrical voltage dip from different controllers. (a) Single sequence FOC controller. (b) Dual sequence FOC controller. Graphs from top to bottom are electric torque T_e and dc voltage V_{dc}, respectively.

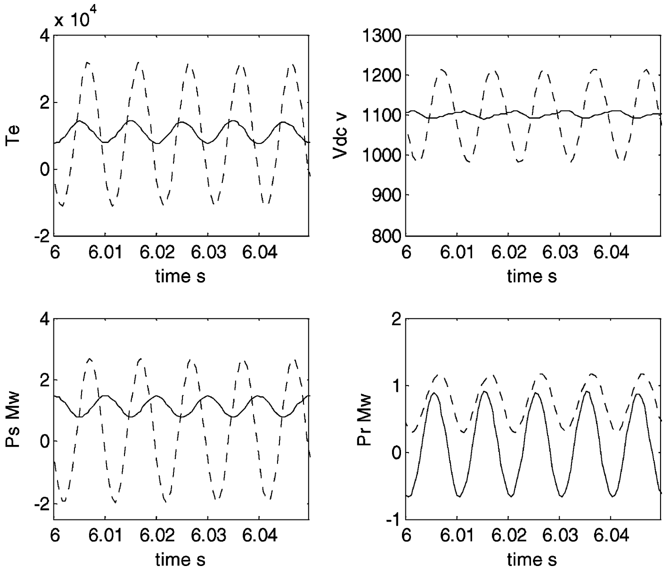

Fig. 12. Compare the responses of DFIG under unsymmetrical voltage dip from different controllers. Dotted line—classical single sequence FOC controller and solid line—proposed dual sequence FOC controller. Graphs from left to right and from top to bottom are electrical torque T_e, dc voltage $V_{\rm dc}$, stator power Ps, and grid VSC power Pconv, respectively.

oscillation increases a little bit. As the stator power often dominates the total power of the generator, the total power oscillation is still limited a lot.

When the grid VSC is controlled separately in positive and negative sequences, and in coordination with the rotor VSC, the dc voltage ripple is drastically limited to less than 10% of the original value. The instantaneous active power of grid VSC is intentionally to be controlled to have a second-order harmonic, in order to compensate the rotor power oscillation $\tilde{p}_{\sin 2\theta}$ and $\tilde{p}_{\cos 2\theta}$.

Under unbalanced grid voltage condition, the classical controller of rotor and grid VSC has to be tuned very fast to limit torque pulsation and dc link voltage ripple and its stability margin will therefore decrease.

V. Conclusion and Recommendation

The LVRT capability of DFIG under symmetrical voltage dip has been thoroughly investigated in many researches, while DFIG's behavior under unsymmetrical voltage dip is seldom studied. Instead of the large transient rotor current caused by the symmetrical voltage dip, the large electric torque pulsation and dc voltage ripple in back-to-back VSCs are identified as the most severe problems of DFIG under unsymmetrical voltage dip. In this paper, the DFIG is proposed to be controlled in dual sequence—positive and negative sequences independently. In order to implement the separated positive and negative sequence controllers of DFIG, two methods to separate positive and negative sequences in real time are compared. The "signal delay cancellation" is much faster than the "low-pass filter," and is chosen in this study. Equations of instantaneous active p and reactive power q, and voltage equations of DFIG and grid VSC in positive *dq* and negative *dq* sequence are derived. The complete DFIG system with the proposed controller is modeled in MATLAB/Simulink. The simulation results prove that the independent positive and negative sequence controllers of rotor VSC and grid VSC effectively limit the electric torque pulsation and dc voltage ripple.

In this paper, the control objective is focused on how to improve the performance of DFIG itself under unsymmetrical voltage, integrated with a strong power grid. In future, the control objective can be focused on how to use DFIG to improve grid performance when it is connected with a weak power grid, such as to limit the grid voltage unbalance, etc.

References

[1] T. Ackermann, *Wind Power in Power Systems*. Hoboken, NJ: Wiley, 2005 (ISBN: 0-470-85508-8).

[2] W. V. Lyon, *Transient Analysis of Alternating Current Machinery. An Application of the Methods of Symmetrical Components*. New York: Wiley, 1954.

[3] J. Morren, J. T. G. Pierik, S. W. H. de Haan, and J. Bozelie, "Grid interaction of offshore wind farms. Part 1. Models for dynamic simulation," *Wind Energy*, vol. 8, no. 3, pp. 279–293, Jul./Sep. 2005.

[4] J. Pierik, J. Morren, E. J. Wiggelinkhuizen, S. W. H. de Haan, T. G. van Engelen, and J. Bozelie, "Electrical and control aspects of offshore wind farms II (Erao II), offshore wind farm case studies," Energy Res. Center of The Netherlands, Petten, The Netherlands, Tech. Rep. ECN&TUD, ECN-C-04-051, 2004, vol. 2.

[5] V. Akhmatov, "Analysis of dynamic behavior of electric power systems with large amount of wind power," Ph.D. dissertation, Electr. Power Eng., Tech. Univ., Copenhagen, Denmark, Apr. 2003 (ISBN: 87-91184-18-5).

[6] A. Petersson, "Analysis, modeling and control of doubly-fed induction generators for wind turbines," Ph.D. dissertation, Electr. Power Eng., Chalmers Univ. Technol., Göteborg, Sweden, 2005.

[7] F. Jiang, Z. Q. Bo, and R. Li, "Performance of induction generator in parallel with an unbalanced three phase system," in *Proc. 1998, POWERCON*, 18–21 Aug., vol. 2, pp. 1193–1197.

[8] B. I. Naess, T. M. Undeland, and T. Gjengedal, "Methods for reduction of voltage unbalance in weak grids connected to wind plants," in *Proc. IEEE Workshop Wind Power Impacts Power Syst.*, Oslo, Norway, Jun. 2002, pp. 1–7.

[9] L. Holdsworth, X. G. Wu, and J. B. Ekanayake, "Comparison of fixed speed and doubly fed induction wind turbines during power system disturbances," *Proc. Inst. Eelect. Eng. Generation, Transm. Distrib.*, vol. 150, no. 3, pp. 343–352, May 2003.

[10] H. A. Kim, "The instantaneous power theory based on mapping matrices in three-phase four-wire systems," in *Proc. Power Convers. Conf.*, Nagaoka, Japan, Aug.1997, vol. 1, pp. 361–366.

[11] N. Akira and T. Tanaka, "A new definition of instantaneous active-reactive current and power based on instantaneous space vectors on polar coordinates in three-phase circuits," *IEEE Trans. Power Del.*, vol. 11, no. 3, pp. 1238–1343, Jul. 1996.

[12] J. S. Saccomando, "Transient operation of grid-connected voltage source converter under unbalanced voltage conditions," in *Proc. Ind. Appl. Conf., 36th IAS Annu. Meeting*, 2001, vol. 4, pp. 2419–2424.

[13] G. D. Marques, "A comparison of active power filter control methods in unbalanced and non-sinusoidal conditions," in *Proc. 24th Annu. Conf. IEEE Ind. Electron. Soc.*, 1998, vol. 1, pp. 444–449.

[14] P. Rioual, H. Pouliquen, and J.-P. Louis, "Regulation of a PWM rectifier in the unbalanced network state using a generalized model," *IEEE Trans. Power Electron.*, vol. 11, no. 3, pp. 495–502, May 1996.

[15] H. S. Song and K. Nam, "Dual current control scheme for PWM converter under unbalanced input voltage conditions," *IEEE Trans. Ind. Electron.*, vol. 46, no. 5, pp. 953–959, Oct. 1999.

[16] T. K. A. Brekken and N. Mohan, "Control of a doubly fed induction wind generator under unbalanced grid voltage conditions," *IEEE Trans. Energy Convers.*, vol. 22, no. 1, pp. 129–135, Mar. 2007.

[17] R. Pena, R. Cardenas, J. Clare, and P. Wheeler, "Control system for unbalanced operation of stand-alone doubly fed induction generators," *IEEE Trans. Energy Convers.*, vol. 22, no. 2, pp. 544–545, Jun. 2007.

[18] A. Petersson, T. Thiringer, L. Harnefors, and T. Petru, “Modeling and experimental verification of grid interaction of a DFIG wind turbine,” *IEEE Trans. Energy Convers.*, vol. 20, no. 4, pp. 878–886, Dec. 2005.

[19] S. Seman, J. Niiranen, and A. Arkkio, “Ride-through analysis of doubly fed induction wind-power generator under unsymmetrical network disturbance,” *IEEE Trans. Power Syst.*, vol. 21, no. 4, pp. 1782–1789, Nov. 2006.

[20] Y. Zhou, P. Bauer, J. Pierik, and J. A. Ferreira, “Control of DFIG under unsymmetrical voltage dip,” in *Proc. Power Electron. Spec. Conf.*, Orlando, FL, Jun. 2007, pp. 933–938.

Yi Zhou (S’04) received the B.Sc. degree in electrical engineering from Zhejiang University, Hangzhou, China, in 1995, and the M.Sc. degree in electric power engineering in 2004 from Delft University of Technology (TU Delft), Delft, The Netherlands, where he has been working toward the Ph.D. degree within the Electric Power Processing Group since 2006.

From 1995 to 2002, he was with Anhui Electric Power Company, where he was engaged in the field on power system analysis, including power flow calculation, stability analysis, and short-term power system planning. His current research interests include power system analysis and grid integration of renewable energy sources.

Paul Bauer (SM’07) received the Master’s degree in electrical engineering from the Technical University of Kosice (TU Kosice), Kosice, Slovakia, in 1985, the Ph.D. degree from Delft University of Technology, Delft, The Netherlands, in 1995, and the title of full professor at Brno University of Technology from the President of Czech Republic, in 2008.

From 1985 to 1990, he was with TU Kosice. Since 1990, he has been with Delft University of Technology, where he is currently an Associate Professor, engaged in power electronics, electrical drives and related subjects. From 2002 to 2003, he was at KEMA, Arnhem, engaged in different projects related to power electronic application in power systems. He is the author or coauthor of more than 40 journal and 170 conference papers, and five books. He is the holder of international patents, and had organized several tutorials at the international conferences such as European Power Electronics (EPE) and power conversion intelligent motion (PCIM) concerning simulation of power electronics, power electronic applications in electrical power systems, and also wind energy. He has worked on many projects for industry concerning wind power, power electronic applications for power systems such as Smarttrafo, etc., and participated in and coordinated several Leonardo da Vinci European Union (EU) projects.

Dr. Bauer is the Chapter Officer of Benelux IEEE Joint Industry Applications Society, the Power Electronics and Power Engineering Society Chapter, and a member of the EPE and the International Steering Committee at numerous conferences. He is a reviewer of different IEEE Transactions and Journals. He organized several panel and forum discussions at the different conferences, and served as invited speaker as well as organized different special sessions.

Jan A. Ferreira (F’05) was born in Pretoria, South Africa, in 1958. He received the B.Sc.Eng. (*cum laude*), M.Sc.Eng. (*cum laude*), and Ph.D. degrees in electrical engineering from Rand Afrikaans University, Johannesburg, South Africa, in 1980, 1982, and 1988, respectively.

During 1981, he was with the Institute of Power Electronics and Electric Drives, Technical University of Aachen, Aachen, Germany. From 1982 to 1985, he was at ESD Pty Ltd. From 1986 to 1997, he was with the Faculty of Engineering, Rand Afrikaans University, where he was the Carl and Emily Fuchs Chair of Power Electronics. Since 1998, he has been a Professor in the Electrical Power Processing Group, Delft University of Technology, Delft, The Netherlands.

Prof. Ferreira was the Chairman of the South African Section of the IEEE from 1993 to 1994. He is the Founding Chairman of the IEEE Joint Industry Applications Society (IAS)/Power Electronics Society (PELS) Benelux Chapter. He was the Transactions Review Chairman of the IEEE IAS Power Electronic Devices and Components Committee, and is an Associate Editor of the IEEE TRANSACTIONS ON POWER ELECTRONICS. He was a member of the IEEE PELS Adcom. He was the Chairman of the CIGRE SC14 National Committee of the Netherlands, and a member of the Executive Committee of the EPE Society. He is currently the Treasurer of the IEEE PELS.

Jan Pierik was born in The Netherlands in 1954. He received the M.Sc. degree in chemical engineering from the Technical University Twente, Enschede, The Netherlands, in 1978.

Since 1980, he has been with the Energy Research Centre of the Netherlands (ECN), Petten, The Netherlands, where he is currently a Senior Research Scientist. His current research interests include modeling and control of electrical systems for wind turbines and wind farms.